

# A LENSLESS, AUTOMATED MICROSCOPE FOR DISEASE DIAGNOSTICS

S. Hugo\*, T. Naidoo\*, H. Swart\*, S. Potgieter\*, P. van Rooyen\* and K. Land\*

\* *Materials Science and Manufacturing, CSIR, PO Box 395, Pretoria, South Africa E-mail: [shugo@csir.co.za](mailto:shugo@csir.co.za).*

**Abstract:** Optical microscopy is widely accepted as one of the gold standards in disease diagnosis. However, factors such as cost and the need for a trained eye limit the prevalence of such equipment, particularly in resource-limited areas such as rural clinics. Lensless microscopy, which is based on principles of digital holography, has illustrated the possibility of using simple and cheap optical components combined with software algorithms to implement microscope platforms. We present a digital in-line holographic microscope (DIHM) platform to be used with image processing and classification algorithms to provide a low cost, portable and automated microscope. Initial results show that the images obtained using the DIHM platform are similar to those obtained using a conventional bright field microscope. Applications of this work are targeted towards the implementation of a full blood count, which could provide resource-limited areas with improved healthcare facilities and diagnosis times.

**Key words:** Microscopy, point-of-care disease diagnostics, digital in-line holographic microscopy.

## 1. INTRODUCTION

### 1.1 Background

The concept of holography dates back to 1948, with its name derived from the Greek words “holos” and “graphein”, meaning entire and to write, respectively [1]. A hologram is a recorded interference pattern between a reference wave and a wave field scattered from an object. Traditionally, holographic plates were used as recording mechanisms to capture the hologram. The recorded holographic image is then illuminated with the reference wave to obtain a reconstructed object wave, which is the same as the original object wave.

Throughout the last few decades, significant developments in the field of holography have been made, particularly with the direct recording of Fresnel holograms, made possible with charge-coupled devices (CCDs) [2]. This method enables full digital recording and processing of holograms, without having to use photographic recording processes. The technique has been labelled direct holography, and more recently, digital holography.

In digital holography, the interference between a reference wave and a scattered wave from an object are captured at the surface of a CCD, or other similar light-sensitive electronic device. The resulting hologram is thus electronically recorded and stored. Numerical reconstruction of the object from the electronically recorded hologram can then be performed. Numerical reconstruction can be implemented using approximations of diffraction theory calculations, e.g. the Fresnel-Kirchoff integral.

Digital holography has seen many improvements and has been applied to a variety of measurement tasks, including

shape measurement and deformation analysis, encryption of information, etc. [1]. Included in these applications is the use of digital holography in imaging, and in particular microscopy [3 - 5], providing microscope systems with a large field of view compared to conventional bright field microscopes.

### 1.2 Motivation and objectives

Digital holography demonstrates the implementation of microscopy methods using simple recording devices (e.g. CCDs), without the need for specialised optical components such as lenses. This illustrates the possibility of using simple and cheap optical components with software algorithms to create a low cost and compact microscope platform.

In addition to the advantages of digital holography for microscopy applications in terms of cost and complexity, digital holography also provides advantages over conventional microscope systems in terms of field of view and depth of field. Digital holography allows for images with a large field of view to be captured, where the field of view is proportional to the size of the digital sensor. In terms of depth of field, conventional microscopes provide a focussed image at a single plane, whereas a hologram contains the complete three-dimensional information of the optical wavefront. This allows for reconstruction of the object image at any focal plane.

Optical microscopy is an established field with vast applications. Among the most important applications is that it is considered one of the gold standards for medical diagnosis, with use in advanced laboratories through to rural clinics. However, conventional optical microscopy makes use of specialised optical components and requires a trained operator.

Implementation of a low cost microscope by means of digital holography techniques could enable microscopy to become a more accessible tool, particularly in resource limited areas. By combining this platform with algorithms for identification of a specific disease to be diagnosed from a biological sample, an automated microscope with a large field of view can be realised, making analysis more efficient. In addition, the reduced complexity of the optics of the digital holography microscopy system would allow for cheaper, more compact and mobile equipment to be developed compared with many traditional microscope systems, potentially providing a point-of-care disease diagnostic solution ideally suited to resource limited settings.

The development of effective point-of-care disease diagnostics, particularly for developing countries, is rapidly becoming a more prominent area of research [6, 7]. The potential impact of such diagnostic tools is high, as there is a global increase in non-communicable and infectious disease, and diagnostics remain expensive and unavailable in areas that are in the greatest need of medical assistance [8].

Applications of this work as a disease diagnostic tool could provide resource limited areas with improved healthcare facilities and reduced diagnosis times without requiring skilled personnel on site. This would be particularly useful and novel in a local South African context, where existing medical diagnostics are generally expensive and thus inaccessible to the majority of the population, with a limited number of trained personnel to operate the diagnostic tools. Other developing countries across the globe, from Africa to Asia, would also benefit from the realisation of a disease diagnostic as presented here, as would developed countries, where point-of-care and home-test medical diagnostics for chronic diseases could be realised.

## 2. PRINCIPLES OF HOLOGRAPHY

Fundamental principles of holography include propagation and interference of light waves, which can be explained using scalar diffraction theory [1, 9].

There are different holography set-ups (off-axis, in-line etc.), many of which have the same theoretical principles [10]. In-line holography with spherical waves is the simplest realisation of the holographic method [3] and will form the basis of the work discussed in this paper.

### 2.1 Hologram generation

The generation of a hologram is illustrated in figure 1. Mathematically, the reference wave,  $E_R$ , with real amplitude,  $A_R$ , and phase,  $\varphi_R$ , is described by

$$E_R(x, y) = A_R(x, y)\exp(j\varphi_R(x, y)) \quad (1)$$

while the object wave,  $E_O$ , with real amplitude,  $A_O$ , and phase,  $\varphi_O$ , is described by

$$E_O(x, y) = A_O(x, y)\exp(i\varphi_O(x, y)) \quad (2)$$

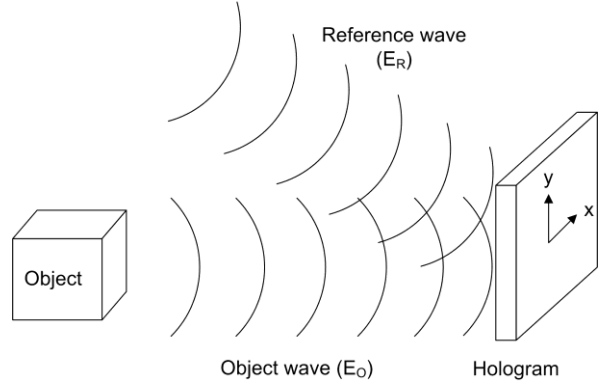


Figure 1: Illustration of hologram generation

The interference of the reference and object waves at the surface of the recording medium has an intensity,  $I(x, y)$ , that represents the hologram. This can be calculated by

$$\begin{aligned} I(x, y) &= |E_O(x, y) + E_R(x, y)|^2 \quad (3) \\ &= E_O(x, y)E_O^*(x, y) + E_R(x, y)E_R^*(x, y) \\ &\quad + E_O(x, y)E_R^*(x, y) + E_R(x, y)E_O^*(x, y) \end{aligned}$$

### 2.2 Image reconstruction from hologram

A hologram of an object that is situated at a distance  $z$  from the recording device (e.g. CCD) can be used to reconstruct a virtual image of the object at the position of the original object. A real image of the object is also formed at a distance  $z$  from the recording device, but in the opposite direction of the recording device. This is illustrated in figure 2. For reconstruction of the undistorted real image at the position previously occupied by the object during recording, the conjugate reference beam is used to illuminate the hologram and obtain a reconstructed image of the object.

For image reconstruction, the diffraction of a light wave at an aperture is calculated. In this case, the hologram is the aperture, and the light wave is the conjugate reference beam, which is assumed to be perpendicular to the hologram.

This is the in-line digital holography set-up. The diffraction can be described quantitatively by the Fresnel-Kirchoff integral in equations (4) to (6). Equation (4) forms the basis for numerical hologram reconstruction. It should be noted that the spherical reference wave is assumed to be far enough from the object to have planar

properties, and thus the conjugate reference beam is equivalent to the reference beam:  $E_R^* = E_R \equiv A_R$ .

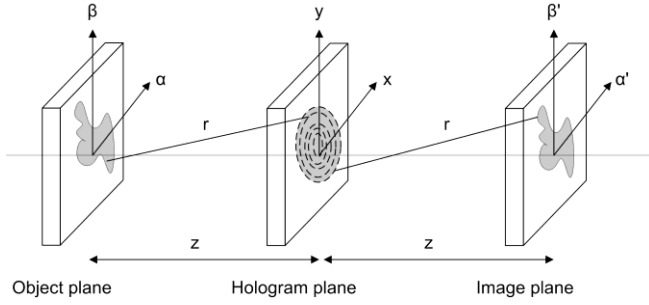


Figure 2: Illustration of coordinate system for hologram reconstruction. Image adapted from [1]

$$I(\alpha', \beta') = \frac{j}{\lambda} \int_{-\infty-\infty}^{\infty} \int_{-\infty-\infty}^{\infty} h(x, y) E_R(x, y) \frac{e^{-jkr'}}{r'} dx dy \quad (4)$$

with

$$r' = \sqrt{(x - \alpha')^2 + (y - \beta')^2 + z^2} \quad (5)$$

and

$$k = \frac{2\pi}{\lambda} \quad (6)$$

### 2.3 Numerical reconstruction

Numerical approximations can be implemented to calculate the Fresnel-Kirchhoff integral for reconstruction of the image. A commonly used technique is the Fresnel approximation, which is used in this work as it is valid for microscopy applications where the object dimensions are small compared to the distance  $z$ .

Equation (5) can be approximated by a Taylor series [1, 9], which enables equation (4) to be modified to the Fresnel approximation or Fresnel transformation as given by equation (7). The double integral can be recognised as a Fourier transform, simplifying the numerical calculation for image reconstruction.

$$I(\alpha', \beta') = \frac{j}{\lambda z} \exp(-jkz) \exp\left(-j \frac{\pi}{\lambda z} (\alpha'^2 + \beta'^2)\right) \times \int_{-\infty-\infty}^{\infty} \int_{-\infty-\infty}^{\infty} E_R(x, y) h(x, y) \exp\left(-j \frac{\pi}{\lambda z} (x^2 + y^2)\right) \exp\left(-j \frac{\pi}{\lambda z} (x\alpha' + y\beta')\right) dx dy \quad (7)$$

### 3. DIGITAL IN-LINE HOLOGRAPHIC MICROSCOPE (DIHM) PLATFORM

The digital in-line holographic microscope (DIHM) platform that was implemented makes use of a laser diode light source, an aperture, and a complimentary metal oxide semiconductor (CMOS) image sensor. A digital hologram of the object being investigated is captured by the image sensor. Image reconstruction is then performed on the hologram to provide an image of the object with a large field of view. CMOS sensors, such as those found in mobile cameras, are readily available and can be utilised for digital microscopy applications, providing a lensless system that is low in cost.

To construct the DIHM platform, interchangeable light sources are used. An infrared laser diode (808 nm) (L808P010, Thorlabs) and a blue laser diode (408 nm) (ML320G2, Thorlabs) have been used. An aperture of 50  $\mu\text{m}$  was used to improve the coherence of the light. The object to be imaged was mounted on a glass microscope slide with dimensions 76 mm x 26 mm x 1 mm. The slide contained either a printed microscopic image, or a stained and fixed blood film, as prepared by pathologist laboratories. The image sensor used was a 1/2.5-Inch 5MP CMOS digital image sensor (MT9P031, Aptina) with a 2.2  $\mu\text{m}$  x 2.2  $\mu\text{m}$  pixel size. The DIHM platform was set up in such a way that the distance  $d$  between the aperture at the light source and the object was 200 mm to ensure a planar wave at the object plane. The distance  $z$  between the object and the image sensor was set at 2 mm. Figure 3 provides a simple illustration of the DIHM platform set-up with the various components and parameters of the system and figure 4 shows the physical experimental set-up that was manufactured.

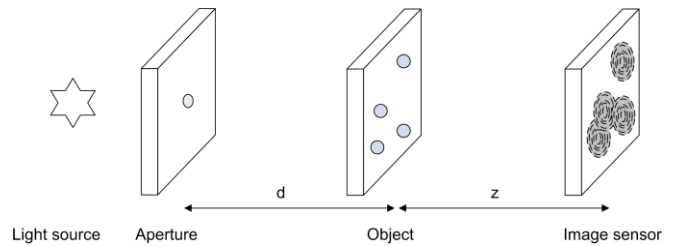


Figure 3: Illustration of DIHM platform components and parameters

### 4. SIMULATIONS

An algorithm was implemented in Matlab to simulate the wave propagation and hologram formation as generated by the physical DIHM platform. The simulation of the wave propagation parameterizes and closely models the physical experimental platform and enables diffraction patterns and holograms of arbitrary objects of a microscopic scale to be generated. This provides a simulation tool that enables parallel testing and optimization of the physical DIHM platform parameters.

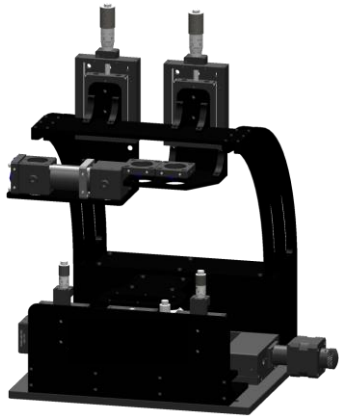


Figure 4: Mechanical design of experimental DIHM platform

## 5. RESULTS

### 5.1 Simulation results

The set of images in figures 5 to 7 show results of a forward wave propagation simulation using an artificial object. The artificial object has a diameter of  $50\ \mu\text{m}$  with smaller irregular shapes inside, similar to the structure of a white blood cell found in human blood.

The model simulates the propagation of a defined light source through the object to create a diffraction pattern (not shown) and a hologram of the object as shown in figure 6. The hologram is then used to reconstruct an image of the original object and the result is shown in figure 7.

The reconstruction algorithm uses as an input either an image of a hologram produced by the wave propagation simulation, as in figure 7, or a hologram image produced by the experimental DIHM platform (figures 8 and 9). The reconstruction algorithm then generates an in focus image of the original object.

### 5.2 Experimental DIHM results

Once simulations of hologram generation and image reconstruction were verified for an artificial object, holograms were recorded using the DIHM platform. As an initial test, a positive 1951 United States Air Force (USAF) Wheel Pattern Test Target slide (R3L1S4P, Thorlabs) was used as the object, with lines and numbering in varying sizes, with the smallest feature sizes around  $2\ \mu\text{m}$ . The infrared laser was used as the light source, with the set-up as described in section 3. Using these parameters, figure 8(a) shows the digital hologram of the central area of the USAF slide, recorded by the CMOS sensor on the DIHM platform.

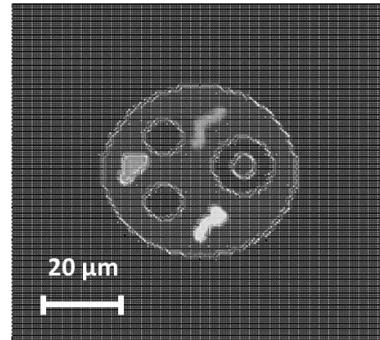


Figure 5: Image of the original simulated object

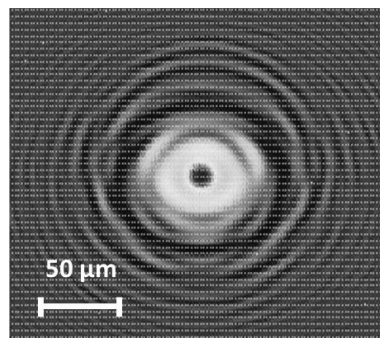


Figure 6: Image of the projected hologram

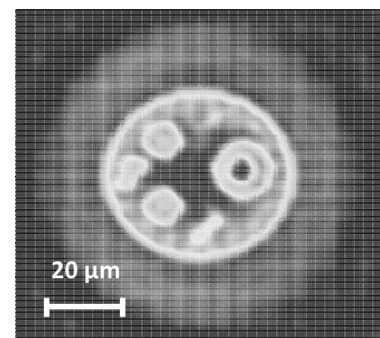
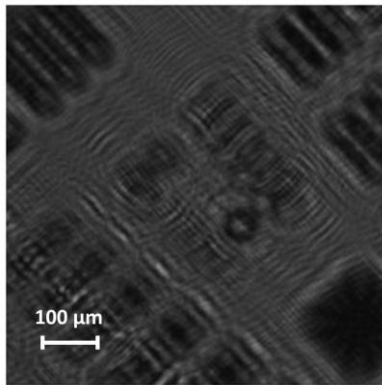


Figure 7: Image of the object reconstruction from the hologram

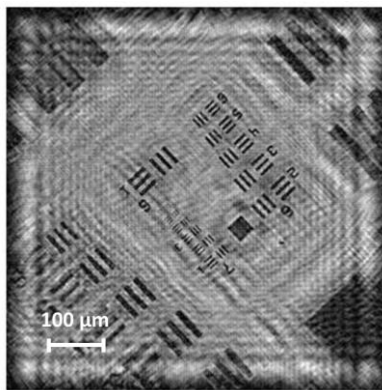
The digital hologram was then used as an input to the image reconstruction algorithm. The algorithm first performs pre-processing of the hologram image by means of a Laplacian filter to enhance the contrast of the hologram. The reconstructed USAF slide image is shown in figure 8(b).

To test the abilities of the DIHM further, blood smear slides were imaged. Experiments were performed with both the infrared and blue laser diodes.

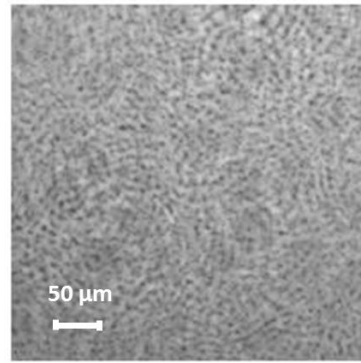




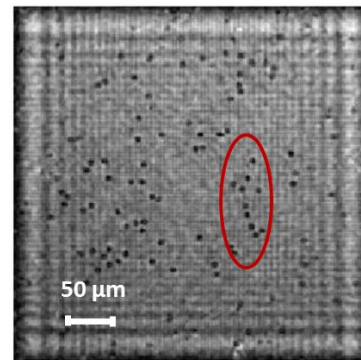
(a)



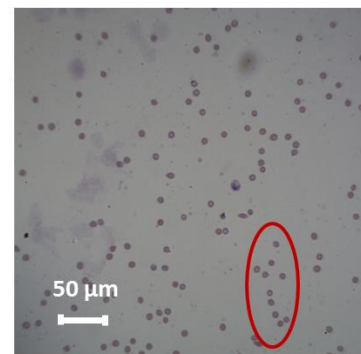
(b)



(a)



(b)



(c)

Figure 8: (a) Hologram of USAF slide obtained using the DIHM platform, and (b) reconstructed image of USAF slide using pre-processed hologram as input to the reconstruction algorithm

A hologram of a small area of a blood film slide that was obtained using a blue laser diode, and other parameters as described in section 3, is shown in figure 9(a). The corresponding reconstructed image is shown in figure 9(b), with a comparison to an image of the same area of the blood film obtained using a conventional bright field microscope with 400X magnification. The circled areas in figure 9(b) and (c) assist in highlighting corresponding areas in the two images.

The abrupt changes at the edges due to the finite sample size of the hologram results in noise at the borders of the reconstructed images in figures 8(b) and 9(b). This can be addressed by using windowing functions. However, initial results obtained indicated that the reconstructed image was of a higher quality when using the cropped images as compared with using standard windowing functions. More advanced and customized windowing techniques could be investigated and implemented to improve the reconstructed image quality.

The blue light source provided clearer results for imaging red blood cells, which are more prevalent than white blood cells in a blood film. This suggests that information from different light sources could be combined for optimal image reconstruction results.

Figure 9: (a) Hologram of blood smear obtained from DIHM, (b) reconstructed image of blood smear, and (c) comparison to image of blood smear obtained using conventional bright field microscope (400 X).

## 6. DISCUSSION

Initial results for both the simulated and experimental DIHM system show the successful implementation of both the physical DIHM platform as well as the reconstruction algorithm.

The implementation of the wave propagation simulations allowed for diffraction patterns and holograms to be generated as a parameter optimisation tool for the DIHM platform, and also enabled the simulations to be verified against existing diffraction theory literature. By using a simple circular aperture through which a light source propagates, the Fraunhofer diffraction pattern or Airy

pattern produced was recorded. The maximum and minimum values along a cross section of the simulated diffraction pattern compared well to expected theoretical values [9] as shown in table 1.

Normalized x values simulated	Normalised x values [9]	Maximum or minimum
0	0	Max
1.187	1.22	Min
1.661	1.635	Max
2.215	2.233	Min
2.69	2.679	Max
3.244	3.238	Min
3.718	3.699	Max

Table 1: Locations of maxima and minima of simulated and theoretical circular aperture diffraction patterns

The diffraction patterns obtained using the wave propagation simulations indicated the successful implementation of the diffraction theory. This shows that the simulations can be used as a tool in investigating diffraction pattern and hologram pattern generation and the parameters required to achieve this.

In addition, since reconstruction of the original image (either simulated or real) was successful using a hologram as an input, this shows that the reconstruction algorithm was successfully implemented.

The reconstruction algorithm provided successful image reconstruction for both simulated artificial objects, as well as real objects where the holograms were recorded using the physical DIHM system. This shows that the physical implementation of the DIHM platform was successfully carried out.

Initial tests to investigate the reconstruction of images of blood cells from a recorded hologram of a blood smear slide have been shown to be successful with a high resolution. Red blood cells are typically 6 – 8  $\mu\text{m}$  in size, and it is clear that the DIHM can resolve these cells (figure 9(b)).

Potential improvements to the DIHM system can be investigated and implemented in terms of physical and image processing techniques. An off-axis set-up as opposed to the in-line digital holography set-up would improve the quality of the reconstructed image, as the reference wave and object waves can be spatially separated and analysed independently. Improvements in the image quality could then further be obtained by using a digital sensor with a smaller pixel size.

The finite sample size or sub-section of the entire hologram used in the image processing of this work does affect the reconstructed image quality. However, [1] demonstrates that the sub-image contains enough of the

hologram information to adequately reconstruct the image. As the sub-image becomes smaller, the quality of the reconstructed image will deteriorate. The optimal size of the sub-section of the hologram could be investigated in future.

A number of image processing techniques have been implemented in this work, including the implementation of a pre-processing Laplacian filter to enhance the contrast of the hologram image before performing image reconstruction. This high frequency filter was found to have the greatest effect on the reconstructed image quality out of all the processing techniques investigated. Smoothing functions were also implemented to soften the noise in the background of the image.

Other image processing techniques investigated included interpolation, stretching, rescaling, and histogram equalisation of the image [11]. The techniques initially investigated were found to have a minimal effect on the quality of the reconstructed image. Further investigation of pre- and post-processing techniques can be carried out in future work to determine the improvements to the reconstructed image quality.

In addition to investigating blood cells and other biological elements for medical imaging, a potential application of the digital holography techniques implemented in this work would be the inspection of micro-defects, which would find use in various manufacturing fields.

## 7. CONCLUSION

Initial results show that the DIHM system produces similar images to those obtained with a conventional bright field microscope. Using this successful lensless imaging system as a basis, the system can be further developed to perform automated identification and counting of the objects being investigated. For example, an initial application of this work will be targeted towards the implementation of an automated full blood count, which could provide resource limited areas with improved healthcare facilities and reduced diagnosis times at a low cost.

## 8. REFERENCES

- [1] U. Schnars and W. Jüptner: *Digital Holography: Digital Hologram Recording, Numerical Reconstruction, and Related Techniques*, Springer-Verlag, Germany, first edition, chapter 1-3 pp. 1-69, 2005.
- [2] U. Schnars and W. Jüptner: "Direct recording of holograms by a CCD-target and numerical Reconstruction", *Applied Optics*, Vol. 33 No. 2, pp. 179-181, 1994.

- [3] J. Garcia-Sucerquia, W. Xu, S. Jericho, P. Klages, M. Jericho and H. Kreuzer: “Digital in-line holographic microscopy”, *Applied Optics*, Vol. 45 No. 5, pp. 836-850, February 2006.
- [4] A. Ozcan and U. Demirci: “Ultra wide-field lens-free monitoring of cells on-chip”, *Lab on a Chip*, Vol. 8, pp. 98-106, 2008.
- [5] W. Bishara, T.-W. Su, A.F. Coskun and A. Ozcan: “Lensfree on-chip microscopy over a wide field-of-view using pixel super-resolution”, *Optics Express*, Vol. 18, No. 11, pp. 11181-11191, May 2010.
- [6] W. Lee, Y.-G. Kim, B. Chung, U. Demirci and A. Khademhosseini: “Nano/Microfluidics for diagnosis of infectious diseases in developing countries”, *Advanced Drug Delivery Reviews*, Vo. 62, pp. 449-457, 2010.
- [7] P. Yager, G.J. Domingo and J. Gerdes: “Point-of-care diagnostics for global health”, *Annual Review of Biomedical Engineering*, Vol 10, pp. 107–144, 2008.
- [8] “Mobile Applications on Health and Learning”, *United Nations Department of Economic and Social Affairs, Division for Public Administration and Development Management, Compendium of ICT Applications on Electronic Government* , New York, Vol. 1., 2007.
- [9] J.W. Goodman: *Introduction to Fourier Optics*, McGraw- Hill, Inc., second edition, chapter 3-4 pp. 32-89, 1996.
- [10] M. Kim: “Principles and techniques of digital holographic microscopy”, *SPIE Reviews*, Vol. 1, pp. 1 – 50, 2010.
- [11] R.C. Gonzalez and R.E. Woods: *Digital Image Processing*, Prentice-Hall, Inc., second edition, chapter 3-5 pp.75-281, 2002.